

Communication

# Luminescent Solar Concentrators from Waterborne Polymer Coatings

Pierpaolo Minei <sup>1</sup>, Giuseppe Iasilli <sup>1</sup>, Giacomo Ruggeri <sup>1,2</sup> and Andrea Pucci <sup>1,2,\*</sup> 

<sup>1</sup> Dipartimento di Chimica e Chimica Industriale, Università di Pisa, Via Giuseppe Moruzzi 13, 56124 Pisa, Italy; pierminei@gmail.com (P.M.); giuseppe.iasilli@gmail.com (G.I.); giacomo.ruggeri@unipi.it (G.R.)

<sup>2</sup> INSTM, UdR Pisa, Via Giuseppe Moruzzi 13, 56124 Pisa, Italy

\* Correspondence: andrea.pucci@unipi.it; Tel.: +39-050-2219270

Received: 6 June 2020; Accepted: 7 July 2020; Published: 8 July 2020



**Abstract:** This study reports for the first time the use of waterborne polymers as host matrices for luminescent solar concentrators (LSCs). Notably, three types of waterborne polymer dispersions based either on acrylic acid esters and styrene (Polidisp<sup>®</sup> 7602), acrylic and methacrylic acid esters (Polidisp<sup>®</sup> 7788) or aliphatic polyester-based polyurethane (Tecfin P40) were selected as amorphous coatings over glass substrates. Water soluble Basic Yellow 40 (BY40) and Disperse Red 277 (DR277) were utilized as fluorophores and the derived thin polymer films (100  $\mu\text{m}$ ) were found homogeneous within the dye range of concentration investigated (0.3–2 wt.%). The optical efficiency determination ( $\eta_{\text{opt}}$ ) evidenced LSCs performances close to those collected from benchmark polymethylmethacrylate (PMMA) thin films and Lumogen Red F350 (LR) with the same experimental setup. Noteworthy, maximum  $\eta_{\text{opt}}$  of  $9.5 \pm 0.2$  were recorded for the Polidisp<sup>®</sup> 7602 matrix containing BY40, thus definitely supporting the waterborne polymer matrices for the development of high performance and cost-effective LSCs.

**Keywords:** waterborne polymer dispersions; water soluble fluorophores; luminescent solar concentrators

## 1. Introduction

Luminescent solar concentrators (LSC) have been considered as one of the most effective solution to promote the diffusion of the photovoltaic (PV) systems in the urban environment. Although discovered in 1977 [1] the utilization of the LSC technology has only recently been fueled by the European Directive supporting the concept of Net Zero-Energy Buildings (NZEBs) [2–9]. NZEBs are buildings with zero net energy consumption, that is on an annual basis they balance their energy consumption with the production of renewable energy. Since  $7 \text{ m}^2/\text{kW}$  is the peak power required for NZEBs [10] the use of the LSC-PV systems would be worthwhile for meeting such energy demand especially in view of the possible installation of large LSC on building facades and terraces [10–13]. LSC are glass or plastic slabs able to harvest the incoming sunlight that is collected via fluorescence on their surface, where it is efficiently converted into electric current by PV cells (Figure 1) [14]. Typical LSCs are composed by high quantum yield organic or inorganic fluorophores that are embedded in optically transparent amorphous polymer plates or films with a good visible transparency and stability over time [15,16]. Among polymer matrices, those based on commercially available polymethylmethacrylates (PMMA) or polycarbonates (PC) are the most utilized, due also to their good compatibility with many fluorophores of different type and nature [15]. Moreover, from the perspective of a more sustainable fabrication route, recent approaches have proposed the use of biobased polymers and materials from renewable resources [17]. For example, L-poly(lactic acid) (L-PLA) [18] cellulose nanocrystals [19] fluorescent proteins [20,21] and polyesters [22] have all been lately reported as green alternatives to PMMA.

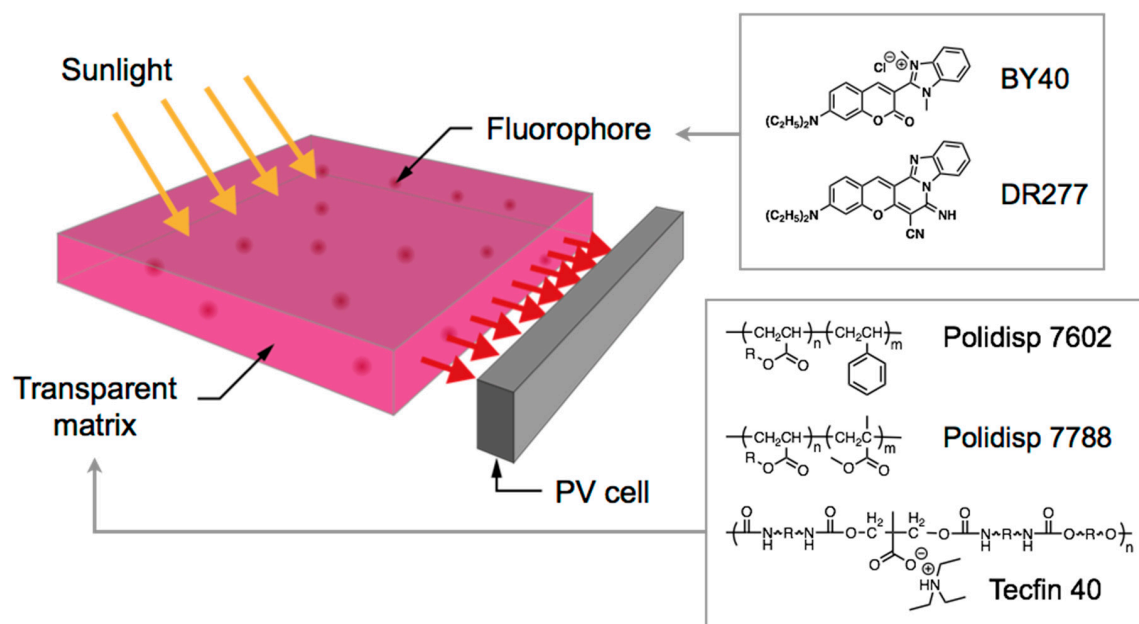


**Figure 1.** Working principle of the LSC-PV system and chemical structure of the investigated fluorophores (BY40 and DR277, inset) as well as the selected polymer matrices.

In connection with these findings, the use of waterborne polymer dispersions is proposed in this work for the realization of thin film LSCs. Waterborne polymers are widely utilized in a range of applications, including paints and coatings, due to their unique properties and the advantage of being solvent free [23–26]. In this work plasticizer-free aqueous copolymer dispersions based on acrylic acid esters and styrene (Polidisp<sup>®</sup> 7602), on acrylic and methacrylic acid esters (Polidisp<sup>®</sup> 7788) and on aliphatic polyester-based polyurethane (Tecfin P40) were selected since they form very homogeneous films over glass surfaces with outstanding weathering resistance. These features have been also confirmed in recent works by our group concerning the preparation of Near-Infrared (NIR) reflective organic coatings [27–29]. Moreover, being water-based, the polymer dispersions minimize the issues associated with the use of toxic volatile organic compounds in the coating process and their eventual disposal costs.

The waterborne dispersions were tested in combination with the water soluble Basic Yellow 40 (BY40) and Disperse Red 277 (DR277) fluorophores (Figure 1). BY40 finds applications in acrylic fibers and in daylight fluorescent pigments [30] and it was selected here thanks to its yellow/green fluorescence, water solubility and excellent compatibility in several media provided by the functional moieties connected to the conjugated central core [31] DR277 is commercially used for the coloration of polyester fabrics for high-visibility safety garments [31,32] and it was eventually tested in LSC as a water soluble molecule in order to validate the proposed approach also by using a red-emitting fluorophore.

All LSCs were obtained by casting the fluorophore-doped waterborne polymer dispersions over optically pure  $50 \times 50 \times 3 \text{ mm}^3$  glass by varying the type of the emitter and its concentration (wt.%), while maintaining constant the film thickness at  $100 \mu\text{m}$ . The performances were determined in terms of the optical efficiency ( $\eta$ ) and discussed with those determined from PMMA-based LSC previously obtained with the same experimental setup [33,34].

## 2. Materials and Methods

### 2.1. Materials

The aqueous copolymer dispersion based on acrylic acid esters and styrene (Polidisp<sup>®</sup> 7602) was supplied by Resiquimica. The milky-like water dispersion is characterized by a pH (25 °C) of 7.5–9, density (20 °C) of  $1.020 \pm 0.010$  g/mL and a solids content of 50 wt.%. The dried material shows a glass transition temperature of about 9 °C. The aqueous copolymer dispersion based on acrylic and methacrylic acid esters (Polidisp<sup>®</sup> 7788) was also supplied by Resiquimica. The milky-like water dispersion is characterized by a pH (25 °C) of 7.5–9, density (20 °C) of  $1.050 \pm 0.010$  g/mL and a solid content of 50 wt.%. The dried material shows a glass transition temperature of about 10 °C. The anionic aliphatic polyester-based polyurethane (Tecfin P40) water dispersion was provided by Tecnochimica Srl. The milky-like water dispersion is characterized by a pH (25 °C) of 7.5–9.5, density (20 °C) of  $1.040 \pm 0.010$  gm/L and a solid content of 30 wt.%. The dried material shows a tensile strength (ASTM D882) of 35–55 MPa. Basic Yellow 40 (BY40, CAS n. 29556-33-0) and Disperse Red 277 (DR277, CAS n. 70294-19-8) were kindly provided by Gruppo Colle (Italy) used without further purification. Poly(methyl methacrylate) (PMMA,  $M_w = 350,000$  g/mol, acid number < 1 mg KOH/g, Aldrich, Milan, Italy) and Lumogen Red F350 (BASF) were used as received. Optically clear glass slides (BOROFLOAT<sup>®</sup> Window, Edmund Optics Ltd., York, UK) were cleaned and dried according to literature methods before their use [22]. The water used to prepare the solutions and dispersions was purified by a Millipore Milli-Q water purification system (Merck, Milan, Italy).

### 2.2. LSC Preparation

A 3 mg/mL stock solution of either BY40 or DR277 in water was prepared. Then, 0.6–0.8 g of waterborne polymer dispersion was diluted with water up to a volume of 1.5 mL and a desired amount of the fluorophore solution added in order to obtain final fluorophore concentrations ranging from 0.3 to 2 wt.%. The dispersion was gently mixed to ensure homogeneity and then casted over  $50 \times 50 \times 3$  mm<sup>3</sup> cleaned glass. Water evaporation was obtained on a warm plate at 40 °C and in a closed environment. Film thickness was measured by means of a micrometer (The L.S. Starrett Company, Athol, MA 01331-1915, USA). LSC based on PMMA thin films and Lumogen Red F350 (LR) were obtained in agreement with literature procedures carried out in our group [22,35–39].

### 2.3. Equipment and techniques

UV-Vis absorption spectroscopy was performed at room temperature by using Cary 5000 spectrophotometer (Agilent, Santa Clara, CA, USA). Fluorescence spectra were measured at room temperature with a Fluorolog<sup>®</sup> -3 spectrofluorometer (Horiba Jobin-Yvon, Horiba Italy, Rome, Italy) equipped with a 450 W xenon arc lamp and double-grating excitation and single-grating emission monochromators. The emission quantum yields were determined by using a 152 mm diameter “Quanta- $\phi$ ” integrating sphere, coated with Spectralon<sup>®</sup> and following recently reported procedures [22,33,34].

The concentration factors and the optical efficiencies of the LSC were obtained by using an <sup>®</sup>LCS-100 solar simulator (ORIEL, Newport, Stratford, CT, USA) under AM 1.5 G simulated solar radiation at an irradiance of 1000 W/m<sup>2</sup> and calibrated by a standard silicon solar cell, and a PV cell (IXYS SLMD121H08L mono solar cell  $86 \times 14$  mm<sup>2</sup>,  $\eta = 22\%$ , the External Quantum Efficiency (EQE) was reported in Figure 2b [36,38,40,41] connected to a precision Keysight Technologies B2900 Series source/measure unit (Keysight Technologies, Santa Rosa, CA, USA). The optical efficiency  $\eta_{\text{opt}}$  was determined from the concentration factor, i.e., the ratio between the short circuit current measured for the cell over the LSC edge ( $I_{\text{LSC}}$ ) and that of the bare cell when perpendicular to the light source ( $I_{\text{SC}}$ ):

$$\eta_{\text{opt}} = \frac{I_{\text{LSC}}}{I_{\text{SC}} \cdot G} \quad (1)$$

where  $G$  is the geometrical factor ( $G = 16.666$ ) that is the ratio between the area exposed to the solar simulator and the collecting area by the PV cell (Figure S1). Notably, during the  $I_{LSC}$  measurements, a white back scattering layer (Microcellular MCPET reflective sheet, ERGA TAPES Srl, Milan, Italy) was placed beneath the LSC with an air gap of about 5 mm. The reported  $\eta_{opt}$  values were calculated as the average of three distinct measurements on identical LSC samples.

### 3. Results and Discussion

Coumarins have been the object of several pioneering works on LSC thanks to their near unity emission quantum yields and excellent compatibility with plastic matrices [42,43]. On this account, Basic Yellow 40 (BY40) and Disperse Red 277 (DR277) were selected as water soluble highly emissive coumarin-based fluorophores and showed absorption maxima centered at 434 and 512 nm, respectively (Figure 2a). For BY40, only a partial fraction of the available range of incident wavelength can be collected [16]. Conversely, thanks to the highly conjugated chromophoric core [44], DR277 showed a broad absorption band that covers most of the solar spectrum characterized by the highest solar irradiance.

The inspection of the emission behavior of BY40 and DR277 revealed fluorescence peaks at 505 (Stokes shift of 71 nm) and 570 nm (Stokes shift of 58 nm), respectively, the latter flanked by an important contribution above 600 nm and in correspondence of the highest external quantum efficiencies (EQE) of the utilized solar PV cell (Figure 2b). Due to their high structural rigidity, both fluorophores have a high quantum yield of fluorescence that reaches values higher than 60%–70% [30,46]. This feature, together with the solar harvesting characteristics (Figure 2a), made the selected fluorophores as good potential candidates for the preparation of efficient luminescent solar concentrators (LSC). Moreover, the Stokes shift higher than 60 nm would also suggest limited auto-absorption phenomena, which are reported to adversely affect the overall performances of LSC [47].

LSCs based on thin films with a thickness of  $100 \pm 10 \mu\text{m}$  were obtained by pouring about 1.5 mL of water dispersion containing 0.6–0.8 g of the waterborne polymer and the desired amount of the fluorophore (0.3 to 2 wt.%) over the  $50 \times 50 \times 3 \text{ mm}^3$  glass substrate. After complete evaporation of the water, very homogeneous thin films were obtained starting from the three different Polidisp<sup>®</sup> 7602, Polidisp<sup>®</sup> 7788 and Tecfin P40 resins with no evident formation of micro-sized dye aggregates (Figure S2). Notably, BY40 was found compatible with all the selected polymer matrices in the investigated interval of concentration, whereas a homogeneous film containing DR277 were obtained from Polidisp<sup>®</sup> 7602 only. As representative examples, photos of the obtained Tecfin P40 thin film containing the 1 wt.% of BY (i.e., 1 wt.% BY/Tecfin P40) are shown in Figure 3 under illumination with a visible and ambient light (Figure 3a) and by using the solar simulator (Figure 3b). Notably, the glass surface appeared homogeneously coated and with a uniform distribution of the fluorophore molecule. Bright and intense fluorescence can be detected, thus suggesting that the selected fluorophores maintained their emission efficiency also when dispersed in the solid Polidisp<sup>®</sup> 7788 and Polidisp<sup>®</sup> 7602 resin films (Figure S3b, for a 1 wt.% BY/Polidisp<sup>®</sup> 7788 and 1 wt.% BY/Polidisp<sup>®</sup> 7602 coatings). The limited dispersability of DR277 in the solid resins were attributed to its more conjugated and rigid chromophoric system than that of BY40 (see Figure 1, inset), which caused a limited interaction with the functional groups of the selected polymer matrices and favored the formation of micro-sized aggregated.

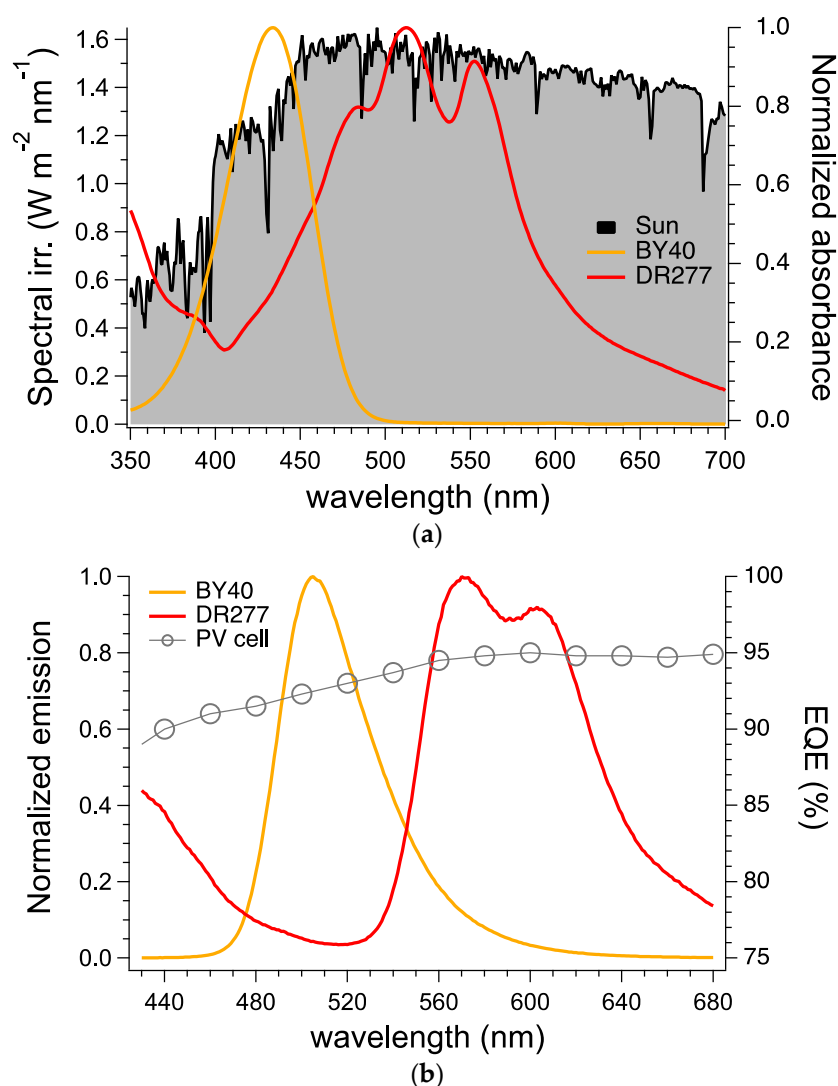


**Figure 2.** (a) Normalized UV-Vis absorption spectra of BY40 (yellow curve) and DR277 (red curve) in water ( $10^{-5}$  M) and solar spectral irradiance at air mass 1.5 (AM 1.5) collected from American Society for Testing and Materials (ASTM). Standard: ASTM G-173-03 [45] (grey curve). (b) Normalized emission spectra of BY40 (yellow curve,  $\lambda_{\text{exc}} = 366$  nm) and DR277 (red curve,  $\lambda_{\text{exc}} = 400$  nm) in water ( $10^{-5}$  M) and external quantum efficiency (EQE, grey open circles) of the utilized PV solar cell.

As a representative example, macroscopic phase segregation can be detected for the 1 wt.% DR277/Tecfin P40 LSC under the illumination of a long-range UV lamp at 366 nm (Figure S4).

The optical performances of the prepared  $50 \times 50 \times 3$  mm<sup>3</sup> LSC were determined in terms of the optical efficiency  $\eta_{\text{opt}}$  that was calculated according to Equation (1) (see Materials and Methods). The concentration factor  $C$  was obtained from the ratio between the short circuit current measured in the case of the cell over the LSC edge ( $I_{\text{LSC}}$ ) and short circuit current of the bare cell when perpendicular to the light source ( $I_{\text{SC}}$ ). Photocurrent measurements were carried out with a home-built device based on a Si-based PV cell attached to one edge of the concentrator (Figure S1) and connected to a source-meter.

Representative  $I/V$  and  $P/V$  curves of the LSC/PV systems based on Polidisp<sup>®</sup> 7602 measured under AM 1.5 G simulated solar irradiation were reported and compared with the same curves obtained from the bare PV cell (Figure 4). In all the investigated LSC/PV systems, both  $I_{\text{LSC}}$  and the maximum power ( $P_{\text{LSC}}$ ) were higher than the respective  $I_{\text{SC}}$  and  $P_{\text{SC}}$ , thus providing concentration factors greater than 1 (Table 1).

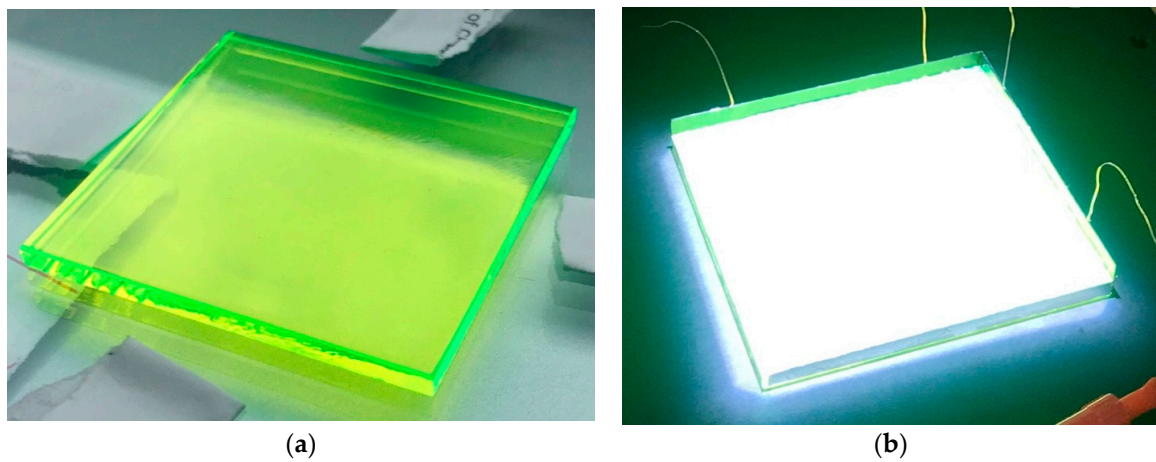


**Figure 3.** (a) Photos of the 1 wt.% BY/Tecfin P40 LSC taken at ambient light and (b) under the illumination of the ORIEL<sup>®</sup> LCS-100 solar simulator lamp. The size of the solar collector is 50 × 50 × 3 mm<sup>3</sup>.

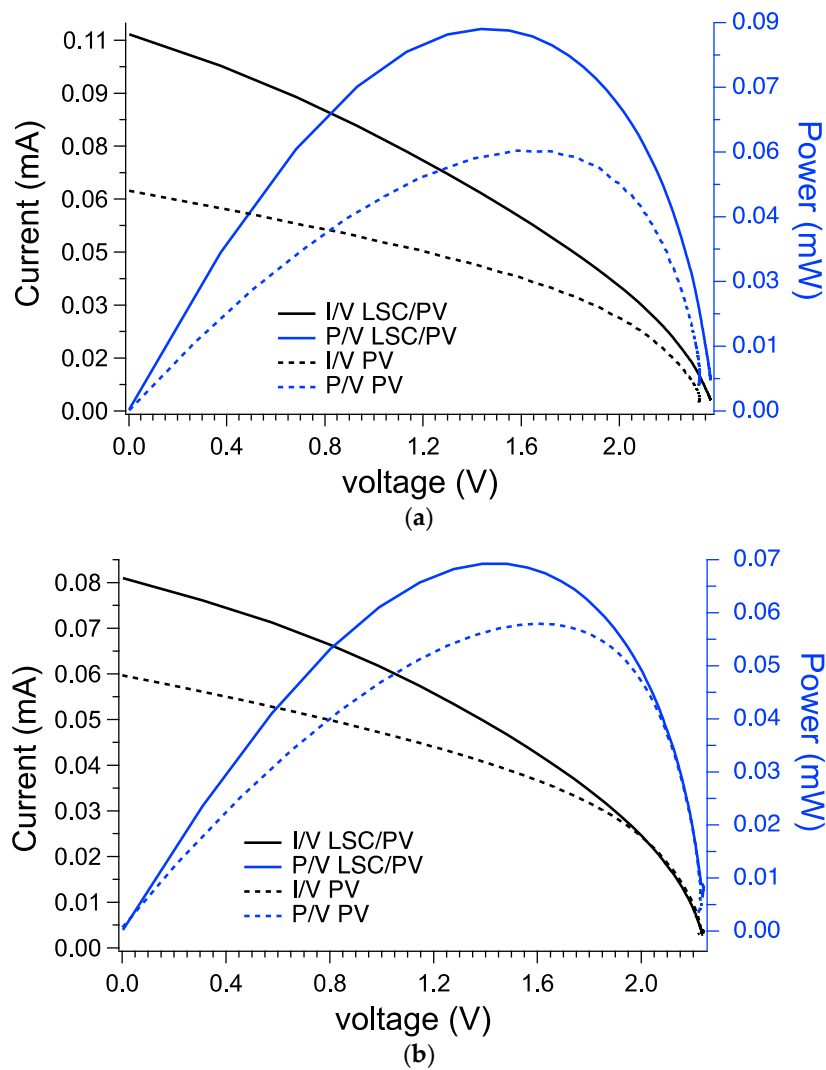


**Figure 4.** Representative I/V (black line) and P/V (blue line) curves obtained for (a) 1.5 wt.% BY40/Polidisp<sup>®</sup> 7602 LSC/PV, (b) 1 wt.% DR277/Polidisp<sup>®</sup> 7602 LSC/PV systems and I/V (black dashed line) and P/V (blue dashed line) curves for the bare PV cell.

The calculated  $C$  and  $\eta_{\text{opt}}$  reported in Table 1, were investigated as a function of the polymer matrix, fluorophore type and its content (wt.%). As far as BY40 is concerned, LSC optical performances increased with fluorophore concentration up to 1.0–1.5 wt.%, after that a decreasing occurred for all the polymer matrices except for Tecfin P40 in which, however, BY40 did not display the highest  $C$  and  $\eta_{\text{opt}}$  values. This peculiar trend was in agreement with the behavior found by Goetzberger who proposed an effective method to evaluate the LSC optical performances as a function of fluorophore content [1,39,48]. Before a certain fluorophore content threshold that depends on its solubility and dispersibility in the polymer matrix, the optical efficiency raising is governed by the solar harvesting features of the LSC system. Namely, more absorbing chromophores are contained and greater are the solar collector performances. Conversely, above that concentration threshold, the optical efficiency of the LSC becomes adversely affected by the typical fluorescence quenching due to the formation of poorly emissive fluorophoric aggregates.

**Table 1.** Concentration factors ( $C$ ) and optical efficiencies ( $\eta_{\text{opt}}$ ) calculated for the prepared LSCs with different fluorophore content (wt.%).  $\eta_{\text{opt}}$  was obtained from  $C$  as an average of 3 measurements ( $G$  factor = 16.666). For LR/PMMA films were selected those with a thickness of  $25 \pm 5 \mu\text{m}$  since they represent those with the highest LSC performances [22,39]. All the measurements were conducted with the same experimental setup.

LSC	Fluorophore Content (wt.%)	$C$	$\eta_{\text{opt}}$ (%)
BY40/Polidisp <sup>®</sup> 7788	0.3	$1.36 \pm 0.01$	$8.2 \pm 0.1$
BY40/Polidisp <sup>®</sup> 7788	0.6	$1.41 \pm 0.01$	$8.5 \pm 0.2$
BY40/Polidisp <sup>®</sup> 7788	1.0	$1.44 \pm 0.01$	$8.6 \pm 0.1$
BY40/Polidisp <sup>®</sup> 7788	1.5	$1.20 \pm 0.01$	$7.2 \pm 0.2$
BY40/Polidisp <sup>®</sup> 7602	0.5	$1.40 \pm 0.01$	$8.5 \pm 0.1$
BY40/Polidisp <sup>®</sup> 7602	1.0	$1.36 \pm 0.01$	$8.2 \pm 0.2$
BY40/Polidisp <sup>®</sup> 7602	1.5	$1.57 \pm 0.01$	$9.5 \pm 0.2$
BY40/Polidisp <sup>®</sup> 7602	2.0	$1.31 \pm 0.01$	$7.9 \pm 0.2$
BY40/Tecfin P40	0.3	$1.18 \pm 0.01$	$7.1 \pm 0.1$
BY40/Tecfin P40	0.5	$1.25 \pm 0.01$	$7.5 \pm 0.1$
BY40/Tecfin P40	0.6	$1.26 \pm 0.01$	$7.6 \pm 0.1$
BY40/Tecfin P40	1.0	$1.29 \pm 0.01$	$7.8 \pm 0.1$
BY40/Tecfin P40	2.0	$1.46 \pm 0.01$	$8.7 \pm 0.2$
DR277/Polidisp <sup>®</sup> 7602	0.5	$1.20 \pm 0.01$	$7.2 \pm 0.1$
DR277/Polidisp <sup>®</sup> 7602	1.0	$1.26 \pm 0.01$	$7.6 \pm 0.2$
DR277/Polidisp <sup>®</sup> 7602	1.5	$1.37 \pm 0.01$	$8.3 \pm 0.3$
DR277/Polidisp <sup>®</sup> 7602	2.0	$1.05 \pm 0.01$	$6.3 \pm 0.2$
LR/PMMA	0.2	$1.14 \pm 0.02$	$6.9 \pm 0.3$
LR/PMMA	0.6	$1.38 \pm 0.03$	$8.3 \pm 0.3$
LR/PMMA	1.0	$1.54 \pm 0.01$	$9.3 \pm 0.2$
LR/PMMA	1.4	$1.69 \pm 0.02$	$10.2 \pm 0.3$
LR/PMMA	1.8	$1.43 \pm 0.02$	$8.6 \pm 0.3$

Polidisp<sup>®</sup> 7602 was revealed as the best polymer matrix since its maximum  $\eta_{\text{opt}}$  of  $9.5 \pm 0.2$  was reached at the BY40 concentration of 1.5 wt.%. This data was notable since it was close to that of  $10.2 \pm 0.3$  calculated for the benchmark LR/PMMA LSC system by using the same experimental setup. This relevant result was attributed to the fact that notwithstanding the lower solar harvesting characteristics and emission not perfectly matching the maximum EQE of the solar cell, the very high dispersibility of BY40 into Polidisp<sup>®</sup> 7602 allowed for maintaining the quantum yield higher than 60% [49] also in the solid state and at the highest wt.% content. Polidisp<sup>®</sup> 7602 being composed by both acrylic acid esters and styrene repeating units possibly enables the generation of effective secondary interactions with BY40 and allowed the fluorophore dispersion when DR277 was used. The solar collecting features of LSCs based on DR277 followed the typical trend with growing  $\eta_{\text{opt}}$  values with fluorophore content. Nevertheless, the lowest  $6.3 \pm 0.2$  optical efficiency calculated for the 2.0 wt.%

DR277/Polidisp<sup>®</sup> 7602 system suggested that significant fluorescence dissipative phenomena occurred at the highest fluorophore content. This behavior was possibly addressed to the highly conjugated and rigid planar structure of DR277 molecules that favored the formation of  $\pi$ - $\pi$  staking interactions that in turn promoted the typical aggregation-caused quenching phenomenon (ACQ) [16,49,50]. Quantum yield of about 30% were actually reported for the DR277/Polidisp<sup>®</sup> 7602 system containing the highest 2 wt.% fluorophore content. This data was even more evident if compared with the performances of the benchmark LR/PMMA LSC systems based on the red-emitting LR fluorophore (Figure 5) that is characterized by a very high compatibility with the acrylic matrix and significant quantum yield also at the highest contents, as reported by many authors in the recent literature as well [39,51–56]. Microscopic investigations actually revealed that no micro-sized or sub-micro-sized assemblies of LR can be detected in the PMMA matrix even at high content [57]. Conversely, compatibility issues (Figure S4) of DR277 adversely affected its homogeneous distribution that resulted detrimental for the optical efficiency of the derived LSC. Anyway, LSC based on the DR277/Polidisp<sup>®</sup> 7602 system provided maximum  $\eta_{opt}$  higher than 8 (i.e.,  $8.3 \pm 0.3$ ), thus confirming the general validity of the proposed idea, that is the preparation of efficient LSC starting from waterborne polymer dispersions.

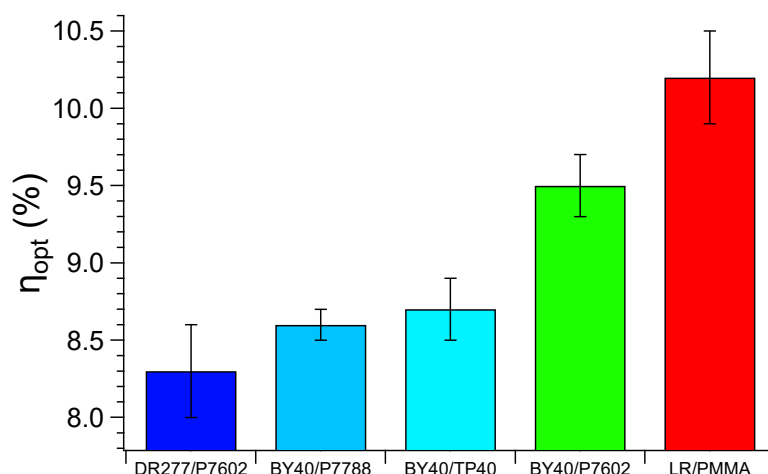


**Figure 5.** Maximum  $\eta_{opt}$  values calculated for the investigated LSC/PV systems. Bars were colored according to the rainbow color table.

The significant optical performances offered by the combination of BY40 with Polidisp<sup>®</sup> 7602 was even more evident when compared in Figure 5 with those maxima of all the investigated LSC/PV systems.

Such a combination appeared very beneficial to boost the diffusion of the LSC/PV technology in the urban environment since the cost of the generated power could be below to the required threshold of 1 €/Watt peak ( $W_p$ ) [58]. For example, the cost of 1 kg of BY40 is estimated to be less than 100 €, whereas 1 kg of LR is quoted about 7,500 € by the BASF chemical company. More than that, the proposed technology could also take advantage of coating techniques typical of paints, thus also decreasing the costs required for the realization of solar collectors with large surface area and those needed for possible renovation due to weathering effects or photodegradation.

#### 4. Conclusions

This work demonstrated the potential of using waterborne polymer matrices such as Polidisp<sup>®</sup> 7602, Polidisp<sup>®</sup> 7788 and Tecfin P40 for replacing benchmark PMMA films in LSC/PV systems. Such matrices were found to uniformly coat glass surfaces and be compatible with the BY40 and DR277 water soluble fluorophores in the investigated 0.3–2 wt.% range of concentrations. The high compatibility, especially that found for BY40 dispersed into Polidisp<sup>®</sup> 7602 possibly provided by the styrenic and acrylic repeating units of the polymer conferred optical performances very close to

those obtained from LR/PMMA thin films in the same range of fluorophore content and experimental setup. Maximum  $\eta_{\text{opt}}$  of  $9.5 \pm 0.2$  were actually obtained, compared with that of  $10.2 \pm 0.3$  obtained from PMMA-based LSCs. These features definitely promoted the waterborne polymer dispersions in combination with the highly emissive water-soluble fluorophores as low cost alternatives for high performance LSCs. Future works will be oriented to finding alternatives to coumarin-based fluorophores that are characterized by limited photostability over long exposure times [16]. Also, fluorophores based on the typical aggregation-induced emission [37,50] will be also taken into account in an attempt to get rid of the typical fluorescence quenching of highly-conjugate red-emitting fluorophores in the solid state.

**Supplementary Materials:** The following are available online at <http://www.mdpi.com/2079-6412/10/7/655/s1>, Figure S1: Home built apparatus for the measurement of the LSC performances; Figure S2: Confocal microscopy image of the 1 wt.% BY/Tecfin P40 LSC; Figure S3: (a) Photos of the 1 wt.% BY/Polidisp<sup>®</sup> 7788 LSC taken at ambient light; (b) under the illumination of a long-range UV lamp at 366 nm; (c) the bare glass under the same UV light; the 1 wt.% BY/Polidisp<sup>®</sup> 7788 taken at ambient light; Figure S4: photo of the 1 wt.% DR277/ Tecfin P40 LSC taken under the illumination of a long-range UV lamp at 366 nm.

**Author Contributions:** Conceptualization, A.P.; methodology, P.M., and G.I.; supervision, G.R.; funding acquisition, A.P. All authors have read and agreed to the published version of the manuscript.

**Funding:** This research was funded by the “Bando Dimostratori Tecnologici” of the University of Pisa.

**Acknowledgments:** Niccolò Pezzati is kindly acknowledged for the preparation of fluorophores dispersions.

**Conflicts of Interest:** The authors declare no conflict of interest.

## References

- Goetzberger, A.; Greube, W. Solar energy conversion with fluorescent collectors. *Appl. Phys.* **1977**, *14*, 123–139. [CrossRef]
- Recast, E. Directive 2010/31/EU of the European Parliament and of the Council of 19 May 2010 on the energy performance of buildings (recast). *Off. J. Eur. Union* **2010**, *18*, 2010.
- Commissie, E. *A Roadmap for Moving to A Competitive Low Carbon Economy in 2050*; Europese Commissie: Brussel, Belgium, 2011.
- Kanellakis, M.; Martinopoulos, G.; Zachariadis, T. European energy policy—A review. *Energy Policy* **2013**, *62*, 1020–1030. [CrossRef]
- Sartori, I.; Napolitano, A.; Voss, K. Net zero energy buildings: A consistent definition framework. *Energy Build.* **2012**, *48*, 220–232. [CrossRef]
- Chai, J.; Huang, P.; Sun, Y. Differential evolution—Based system design optimization for net zero energy buildings under climate change. *Sustain. Cities Soc.* **2020**, *55*, 102037. [CrossRef]
- Kivimaa, P.; Primmer, E.; Lukkarinen, J. Intermediating policy for transitions towards net-zero energy buildings. *Environ. Innov. Soc. Transit.* **2020**. [CrossRef]
- Lin, W.; Ma, Z.; McDowell, C.; Baghi, Y.; Banfield, B. Optimal design of a thermal energy storage system using phase change materials for a net-zero energy Solar Decathlon house. *Energy Build.* **2020**, *208*, 109626. [CrossRef]
- Luo, Y.; Zhang, L.; Liu, Z.; Yu, J.; Xu, X.; Su, X. Towards net zero energy building: The application potential and adaptability of photovoltaic-thermoelectric-battery wall system. *Appl. Energy* **2020**, *258*, 114066. [CrossRef]
- Meinardi, F.; Bruni, F.; Brovelli, S. Luminescent solar concentrators for building-integrated photovoltaics. *Nat. Rev. Mater.* **2017**, *2*, 17072. [CrossRef]
- Armaroli, N.; Balzani, V. Solar electricity and solar fuels: Status and perspectives in the context of the energy transition. *Chem.—Eur. J.* **2016**, *22*, 32–57. [CrossRef]
- Ter Schiphorst, J.; Cheng, M.L.M.K.H.Y.K.; Van Der Heijden, M.; Hageman, R.L.; Bugg, E.L.; Wagenaar, T.J.L.; Debije, M. Printed luminescent solar concentrators: Artistic renewable energy. *Energy Build.* **2020**, *207*. [CrossRef]
- Wiegman, J.; Van der Kolk, E. Building integrated thin film luminescent solar concentrators: Detailed efficiency characterization and light transport modelling. *Sol. Energy Mater. Sol. Cells* **2012**, *103*, 41–47. [CrossRef]

14. Ferreira, R.A.S.; Correia, S.F.H.; Monguzzi, A.; Liu, X.; Meinardi, F. Spectral converters for photovoltaics—What's ahead. *Mater. Today* **2020**, *33*, 105–121. [[CrossRef](#)]
15. Li, Y.; Zhang, X.; Zhang, Y.; Dong, R.; Luscombe, C.K. Review on the role of polymers in luminescent solar concentrators. *J. Polym. Sci. Part A Polym. Chem.* **2019**, *57*, 201–215. [[CrossRef](#)]
16. Beverina, L.; Sanguineti, A. Organic fluorophores for luminescent solar concentrators. *Solar Cell Nanotechnol.* **2013**, 317–355.
17. Li, Z.; Zhao, X.; Huang, C.; Gong, X. Recent advances in green fabrication of luminescent solar concentrators using nontoxic quantum dots as fluorophores. *J. Mater. Chem. C* **2019**, *7*, 12373–12387. [[CrossRef](#)]
18. Fattori, V.; Melucci, M.; Ferrante, L.; Zambianchi, M.; Manet, I.; Oberhauser, W.; Giambastiani, G.; Frediani, M.; Giachi, G.; Camaioni, N. Poly (lactic acid) as a transparent matrix for luminescent solar concentrators: A renewable material for a renewable energy technology. *Energy Environ. Sci.* **2011**, *4*, 2849–2853. [[CrossRef](#)]
19. Chowdhury, F.I.; Dick, C.; Meng, L.; Mahpeykar, S.M.; Ahvazi, B.; Wang, X. Cellulose nanocrystals as host matrix and waveguide materials for recyclable luminescent solar concentrators. *RSC Adv.* **2017**, *7*, 32436–32441. [[CrossRef](#)]
20. Sadeghi, S.; Melikov, R.; Jalali, H.B.; Karatum, O.; Srivastava, S.B.; Conkar, D.; Firat-Karalar, E.N.; Nizamoglu, S. Ecofriendly and efficient luminescent solar concentrators based on fluorescent proteins. *ACS Appl. Mater. Interfaces* **2019**, *11*, 8710–8716. [[CrossRef](#)]
21. Melucci, M.; Durso, M.; Favaretto, L.; Capobianco, M.L.; Benfenati, V.; Sagnella, A.; Ruani, G.; Muccini, M.; Zamboni, R.; Fattori, V.; et al. Silk doped with a bio-modified dye as a viable platform for eco-friendly luminescent solar concentrators. *RSC Adv.* **2012**, *2*, 8610–8613. [[CrossRef](#)]
22. Geervliet, T.A.; Gavrilu, I.; Iasilli, G.; Picchioni, F.; Pucci, A. Luminescent solar concentrators based on renewable polyester matrices. *Chem.–Asian J.* **2019**, *14*, 877–883. [[CrossRef](#)] [[PubMed](#)]
23. Zhou, X.; Li, Y.; Fang, C.; Li, S.; Cheng, Y.; Lei, W.; Meng, X. Recent advances in synthesis of waterborne polyurethane and their application in water-based ink: A review. *J. Mater. Sci. Technol.* **2015**, *31*, 708–722. [[CrossRef](#)]
24. Peruzzo, P.J.; Anbinder, P.S.; Pardini, O.R.; Vega, J.; Costa, C.A.; Galembeck, F.; Amalvy, J.I. Waterborne polyurethane/acrylate: Comparison of hybrid and blend systems. *Prog. Org. Coat.* **2011**, *72*, 429–437. [[CrossRef](#)]
25. Chattopadhyay, D.K.; Raju, K.V.S.N. Structural engineering of polyurethane coatings for high performance applications. *Prog. Polym. Sci. (Oxf.)* **2007**, *32*, 352–418. [[CrossRef](#)]
26. Padget, J.C. Polymers for water-based coatings—A systematic overview. *J. Coat. Technol.* **1994**, *66*, 89–105.
27. Muniz-Miranda, F.; Minei, P.; Contiero, L.; Labat, F.; Ciofini, I.; Adamo, C.; Bellina, F.; Pucci, A. Aggregation effects on pigment coatings: Pigment red 179 as a case study. *ACS Omega* **2019**, *4*, 20315–20323. [[CrossRef](#)]
28. Martini, F.; Minei, P.; Lessi, M.; Contiero, L.; Borsacchi, S.; Ruggeri, G.; Geppi, M.; Bellina, F.; Pucci, A. Structural order and NIR reflective properties of perylene bisimide pigments: Experimental evidences from a combined multi-technique study. *Dye. Pigment.* **2020**, 179. [[CrossRef](#)]
29. Minei, P.; Lessi, M.; Contiero, L.; Borsacchi, S.; Martini, F.; Ruggeri, G.; Geppi, M.; Bellina, F.; Pucci, A. Boosting the NIR reflective properties of perylene organic coatings with thermoplastic hollow microspheres: Optical and structural properties by a multi-technique approach. *Sol. Energy* **2020**, *198*, 689–695. [[CrossRef](#)]
30. Christie, R.M. Fluorescent dyes. In *Handbook of Textile and Industrial Dyeing*; Clark, M., Ed.; Woodhead Publishing: Cambridge, UK, 2011; Volume 1, pp. 562–587.
31. Chapter 3 Phenomena Involving Absorption of Energy Followed by Emission of Light. In *Chromic Phenomena: Technological Applications of Colour Chemistry*, 2nd ed.; The Royal Society of Chemistry: London, UK, 2010; pp. 234–365.
32. Gulrajani, M.L. Disperse dyes. In *Handbook of Textile and Industrial Dyeing*; Clark, M., Ed.; Woodhead Publishing: Cambridge, UK, 2011; Volume 1, pp. 365–394.
33. Albano, G.; Colli, T.; Nucci, L.; Charaf, R.; Biver, T.; Pucci, A.; Aronica, L.A. Synthesis of new bis [1-(thiophenyl) propynones] as potential organic dyes for colorless luminescent solar concentrators (LSCs). *Dye. Pigment.* **2020**, *174*, 108100. [[CrossRef](#)]
34. Albano, G.; Colli, T.; Biver, T.; Aronica, L.A.; Pucci, A. Photophysical properties of new p-phenylene- and benzodithiophene-based fluorophores for luminescent solar concentrators (LSCs). *Dye. Pigment.* **2020**, *178*, 108368. [[CrossRef](#)]

35. Iasilli, G.; Francischello, R.; Lova, P.; Silvano, S.; Surace, A.; Pesce, G.; Alloisio, M.; Patrini, M.; Shimizu, M.; Comoretto, D.; et al. Luminescent solar concentrators: Boosted optical efficiency by polymer dielectric mirrors. *Mater. Chem. Front.* **2019**, *3*, 429–436. [[CrossRef](#)]
36. Mori, R.; Iasilli, G.; Lessi, M.; Munoz-Garcia, A.B.; Pavone, M.; Bellina, F.; Pucci, A. Luminescent solar concentrators based on PMMA films obtained from a red-emitting ATRP initiator. *Polym. Chem.* **2018**, *9*, 1168–1177. [[CrossRef](#)]
37. De Nisi, F.; Francischello, R.; Battisti, A.; Panniello, A.; Fanizza, E.; Striccoli, M.; Gu, X.; Leung, N.L.C.; Tang, B.Z.; Pucci, A. Red-emitting AIEgen for luminescent solar concentrators. *Mater. Chem. Front.* **2017**, *1*, 1406–1412. [[CrossRef](#)]
38. Lucarelli, J.; Lessi, M.; Manzini, C.; Minei, P.; Bellina, F.; Pucci, A. N-alkyl diketopyrrolopyrrole-based fluorophores for luminescent solar concentrators: Effect of the alkyl chain on dye efficiency. *Dye. Pigment.* **2016**, *135*, 154–162. [[CrossRef](#)]
39. Carlotti, M.; Fanizza, E.; Panniello, A.; Pucci, A. A fast and effective procedure for the optical efficiency determination of luminescent solar concentrators. *Sol. Energy* **2015**, *119*, 452–460. [[CrossRef](#)]
40. Sottile, M.; Tomei, G.; Borsacchi, S.; Martini, F.; Geppi, M.; Ruggeri, G.; Pucci, A. Epoxy resin doped with Coumarin 6: Example of accessible luminescent collectors. *Eur. Polym. J.* **2017**, *89*, 23–33. [[CrossRef](#)]
41. Gianfaldoni, F.; De Nisi, F.; Iasilli, G.; Panniello, A.; Fanizza, E.; Striccoli, M.; Ryuse, D.; Shimizu, M.; Biver, T.; Pucci, A. A push-pull silafluorene fluorophore for highly efficient luminescent solar concentrators. *RSC Adv.* **2017**, *7*, 37302–37309. [[CrossRef](#)]
42. Drake, J.M.; Lesiecki, M.L.; Sansregret, J.; Thomas, W.R.L. Organic dyes in PMMA in a planar luminescent solar collector: A performance evaluation. *Appl. Opt.* **1982**, *21*, 2945–2952. [[CrossRef](#)]
43. Batchelder, J.S.; Zewail, A.H.; Cole, T. Luminescent solar concentrators. 2: Experimental and theoretical analysis of their possible efficiencies. *Appl. Opt.* **1981**, *20*, 3733–3754. [[CrossRef](#)]
44. Shinde, S.S.; Sreenath, M.C.; Chitrabalam, S.; Joe, I.H.; Sekar, N. Spectroscopic, DFT and Z-scan approach to study linear and nonlinear optical properties of Disperse Red 277. *Opt. Mater.* **2020**, *99*, 109536. [[CrossRef](#)]
45. *ASTM G-173-03 Standard Tables for Reference Solar Spectral Irradiances: Direct Normal and Hemispherical on 37° Tilted Surface*; ASTM International: West Conshohocken, PA, USA, 2012.
46. Fu, D.; Zhi, W.; Lv, L.; Luo, Y.; Xiong, X.; Kang, X.; Hou, W.; Yan, J.; Zhao, H.; Zheng, L. Construction of ratiometric hydrogen sulfide probe with two reaction sites and its applications in solution and in live cells. *Spectrochim. Acta Part A Mol. Biomol. Spectrosc.* **2020**, *224*, 117391. [[CrossRef](#)] [[PubMed](#)]
47. Debije, M.G.; Verbunt, P.P.C. Thirty years of luminescent solar concentrator research: Solar energy for the built environment. *Adv. Energy Mater.* **2012**, *2*, 12–35. [[CrossRef](#)]
48. Carlotti, M.; Ruggeri, G.; Bellina, F.; Pucci, A. Enhancing optical efficiency of thin-film luminescent solar concentrators by combining energy transfer and stacked design. *J. Lumin.* **2016**, *171*, 215–220. [[CrossRef](#)]
49. Pezzati, N.; Minei, P.; Iasilli, G.; Ruggeri, G.; Pucci, A. Manuscript in preparation.
50. Pucci, A. Luminescent solar concentrators based on aggregation induced emission. *Isr. J. Chem.* **2018**, *58*, 837–844. [[CrossRef](#)]
51. Van Sark, W.G.; Barnham, K.W.; Slooff, L.H.; Chatten, A.J.; Büchtemann, A.; Meyer, A.; McCormack, S.J.; Koole, R.; Farrell, D.J.; Bose, R.; et al. Luminescent solar concentrators—A review of recent results. *Opt. Express* **2008**, *16*, 21773–21792. [[CrossRef](#)]
52. McKenna, B.; Evans, R.C. Towards efficient spectral converters through materials design for luminescent solar devices. *Adv. Mater. (Weinh. Ger.)* **2017**, *29*, 1606491. [[CrossRef](#)]
53. Parola, I.; Zarella, D.; Evert, R.; Kielhorn, J.; Jakobs, F.; Illarramendi, M.A.; Zubia, J.; Kowalsky, W.; Johannes, H.H. High performance fluorescent fiber solar concentrators employing double-doped polymer optical fibers. *Sol. Energy Mater. Sol. Cells* **2018**, *178*, 20–28. [[CrossRef](#)]
54. Griffini, G. Host matrix materials for luminescent solar concentrators: Recent achievements and forthcoming challenges. *Front. Mater.* **2019**, *6*. [[CrossRef](#)]
55. Jakubowski, K.; Huang, C.S.; Gooneie, A.; Boesel, L.F.; Heuberger, M.; Hufenus, R. Luminescent solar concentrators based on melt-spun polymer optical fibers. *Mater. Des.* **2020**, *189*. [[CrossRef](#)]
56. Li, Y.; Sun, Y.; Zhang, Y. Luminescent solar concentrators performing under different light conditions. *Sol. Energy* **2019**, *188*, 1248–1255. [[CrossRef](#)]

57. Credi, C.; Pintossi, D.; Bianchi, C.L.; Levi, M.; Griffini, G.; Turri, S. Combining stereolithography and replica molding: On the way to superhydrophobic polymeric devices for photovoltaics. *Mater. Des.* **2017**, *133*, 143–153. [[CrossRef](#)]
58. Van Sark, W.G.J.H.M. Luminescent solar concentrators—A low cost photovoltaics alternative. *Renew. Energy* **2013**, *49*, 207–210. [[CrossRef](#)]



© 2020 by the authors. Licensee MDPI, Basel, Switzerland. This article is an open access article distributed under the terms and conditions of the Creative Commons Attribution (CC BY) license (<http://creativecommons.org/licenses/by/4.0/>).